Radiation Measurements 142 (2021) 106566

Contents lists available at ScienceDirect

Radiation Measurements

journal homepage: http://www.elsevier.com/locate/radmeas

# Modelling the dependence of equivalent dose determined from a dose recovery test on preheating temperature: The intervention of shallow electron traps

Jun Peng [a,*], Xulong Wang [b,c], Grzegorz Adamiec [d], Vasilis Pagonis [e], Jeong-Heon Choi [f]

[a] School of Resource & Environment and Safety Engineering, Hunan University of Science and Technology, Hunan, Xiangtan, 411201, China
[b] SLLQG, CAS Center for Excellence in Quaternary Science and Global Change, Institute of Earth Environment, Chinese Academy of Sciences, Xi'an, 710061, China
[c] Southern Marine Science and Engineering Guangdong Laboratory (Zhuhai), Zhuhai, 519082, China
[d] Institute of Physics - Centre for Science and Education, Division of Geochronology and Environmental Isotopes, Silesian University of Technology, Konarskiego 22B, 44-100, Gliwice, Poland
[e] McDaniel College, Physics Department, Westminster, MD, 21157, USA
[f] Department of Earth and Environmental Sciences, Korea Basic Science Institute, Ochang Center, Chungbuk, 28119, Republic of Korea

ARTICLE INFO

*Keywords:*
Quartz OSL
Equivalent dose
Dose recovery
Preheating temperature
Shallow electron traps

ABSTRACT

In optically stimulated luminescence (OSL) dating, the performance of the single-aliquot regenerative-dose (SAR) protocol is commonly tested using a dose recovery test. The dependence of equivalent dose ($D_e$) determined in a dose recovery test on preheating temperature using quartz OSL was reported in previous studies which demonstrated that using a lower preheating temperature prior to the measurement of the test dose OSL response may result in serious underestimation of the recovered $D_e$. In this study, we simulate the variation of normalised sensitivity-corrected OSL signals as a function of cycle number and the dependence of the recovered $D_e$ on preheating conditions, using a kinetic model consisting of four electron traps and two recombination centres. Experimentally observed phenomena are successfully reproduced using the model with a set of optimised kinetic parameters. We suggest that the intervention of shallow electron traps may play a significant role in affecting the accuracy of $D_e$ determination. Relevant mechanisms are explained, and implications on dose measurements using the SAR protocol are discussed.

## 1. Introduction

The dose recovery test (Roberts et al., 1999; Murray and Wintle, 2003; Wintle and Murray, 2006) is routinely applied in optically stimulated luminescence (OSL) dating to test the ability of the single-aliquot regenerative-dose (SAR) protocol (Murray and Wintle, 2000) to recover known laboratory doses. During the application of this test, the natural sample is bleached by an optical exposure, then given a laboratory dose serving as the unknown "natural" dose; subsequently the "natural" dose is determined by means of the SAR protocol. Although the dose recovery test does not unequivocally inform whether the natural dose can be measured accurately, it is more sensitive than the recycling ratio in testing whether sensitivity changes among regenerative cycles are successfully corrected (e.g., Murray and Wintle, 2003). However, there are many sources of error (intrinsic and extrinsic factors) that may lead to a variation of the equivalent dose ($D_e$) determined from a dose recovery test for quartz OSL (e.g., Thomsen et al., 2005; Jacobs et al., 2006a). Thomsen et al. (2005) demonstrated a dependence of the recovered $D_e$ on the number of integration channels used for some of their investigated quartz samples. Choi et al. (2009) reported a dependence of the recovered dose on the light sources used to bleach the natural quartz OSL. Wang et al. (2011) found a dependence of recovered $D_e$ on the temperatures used during OSL stimulation, and on the bleaching time used before administering the "natural" dose. Duller (2012) found that the recovered $D_e$ became increasingly underestimated at high doses, if the relative proportion of OSL signal from the non-fast component was large in the initial OSL signal from quartz. Feathers and Pagonis, 2015 demonstrated in a simulation study that large grain-to-grain variation in the decay constant for the fast and medium OSL components could cause the underestimation of the recovered $D_e$.

The preheating before OSL measurements is essential in order to remove the unwanted signals from light sensitive shallow traps, and acts

* Corresponding author.
*E-mail address:* pengjun10@mails.ucas.ac.cn (J. Peng).

https://doi.org/10.1016/j.radmeas.2021.106566
Received 9 June 2020; Received in revised form 6 December 2020; Accepted 5 March 2021
Available online 18 March 2021
1350-4487/© 2021 Elsevier Ltd. All rights reserved.

as the sensitivity equaliser for natural and laboratory irradiated samples. However, preheat temperature dependent underestimation of the recovered $D_e$ for quartz OSL is widely reported in the literature. Bailey (2000) demonstrated a strong dependence of the recovered $D_e$ on the preheating conditions for an annealed and a laboratory irradiated sample. Murray and Wintle (2000) chose to use a preheat (PH) temperature in the range of 160–300 °C (for 10 s) before the measurement of the natural/regenerative OSL responses and to use a cut-heat (CH) temperature of 160 °C before the measurement of the test dose OSL responses during the development of the SAR protocol. However, later it was reported in several studies that it was inappropriate to apply a CH temperature of 160 °C for some samples (e.g., Murray and Wintle, 2003; Choi et al., 2003a, b; Jacobs et al., 2006b). Murray and Wintle (2003) used a CH temperature of 160 °C and found significant recuperation of OSL signals and underestimation of given doses for some samples. They ascribed this to charge in a light-insensitive trap not being cleaned up at the end of the measurement of the test dose OSL signal. Choi et al. (2003a) argued that the presence of a light-sensitive ultrafast OSL component that is thermally unstable was responsible for the poor performance (characterised by large recycling ratio, high recuperation, and significant underestimation of $D_e$) in their SAR dose recovery test when a CH temperature of 160 °C was used. Jacobs et al. (2006b) identified a preferential reduction in a thermally unstable slow OSL component as the CH temperature increased and related the presence of this component to $D_e$ underestimation in their dose recovery tests when a low CH temperature (i.e., 160 °C) was used. Many studies suggested that the underestimation of doses can be resolved by applying a higher CH temperature (e.g., Choi et al., 2003a, b; Jacobs et al., 2006b).

Shallow electron traps are, by definition, relatively unstable (compared to the 325 °C thermoluminescence (TL) trap) and are likely to release electrons thermally at lower temperatures (here defined as 100–300 °C). These electron traps are responsible for several TL glow peaks observed in natural quartz (Aitken, 1985; Spooner and Questiaux, 2000; Pagonis et al., 2002). Three widely observed phenomena closely related to shallow electron traps are the production of phosphorescence (e.g., Jacobs et al., 2006b; Ankjærgaard and Jain, 2010) or isothermal TL (Choi et al., 2003b), thermal transfer (e.g., Rhodes and Bailey, 1997; Wintle and Murray, 2006), and recuperation after bleaching (e.g., Aitken and Smith, 1988) or phototransfer (e.g., Bailiff et al., 1977; Peng and Wang, 2020). It is believed that shallow electron traps exert significant influence on the shape of the OSL decay curves (McKeever et al., 1997a; Chruścińska and Przegiętka, 2010), on the production of thermally dependent OSL signal (Chruścińska and Przegiętka, 2011), on the initial sensitivity changes during single-aliquot procedures (McKeever et al., 1997b), and on the thermally dependent $D_e$ estimates (Kijek et al., 2013; Kijek and Chruścińska, 2015). These effects depend on the preheating temperature and are expected to be eliminated gradually at elevated measurement temperatures, because shallow electron traps become increasingly inactive as the measurement temperature increases (McKeever et al., 1997a).

This study aims at simulating the preheating temperature-dependent variation in $D_e$ in a dose recovery experiment. We perform quantitative modelling on processes involved in irradiation, preheating, and stimulation, as related to various charge competitors, using the experimentally measured results of Choi et al. (2003a) as the basis of the simulation. We emphasise the intervention of shallow electron traps on the reliability of $D_e$ determined in a dose recovery test. The simulation results are directly related to OSL dating and give insights into possible improvements of the SAR protocol on $D_e$ determination.

## 2. Model and methods

The kinetic model used in this study consists of four electron traps and two recombination centres, and is expressed by the following equations:

$$\frac{dn_i}{dt} = A_{ni}(N_i - n_i)n_c - n_i F\sigma_i - n_i s_{ni}\exp\left(-\frac{E_{ni}}{k_B(T_0+\beta t)}\right) \quad i = 1,2,3,4 \tag{1}$$

$$\frac{dm_j}{dt} = A_{mj}(M_j - m_j)n_v - m_j s_{mj}\exp\left(-\frac{E_{mj}}{k_B(T_0+\beta t)}\right) - n_c B_j m_j \quad j = 1,2 \tag{2}$$

$$\frac{dn_c}{dt} = X - \sum_{i=1}^{i=4}\frac{dn_i}{dt} - \sum_{j=1}^{j=2} n_c B_j m_j \tag{3}$$

$$\frac{dn_v}{dt} = X - \sum_{j=1}^{j=2}\frac{dm_j}{dt} - \sum_{j=1}^{j=2} n_c B_j m_j \tag{4}$$

where, $n_i$ and $m_j$ are the trapped electron and hole concentrations ($cm^{-3}$); $n_c$ and $n_v$ the electron and hole concentrations in the conduction and valence bands respectively; $A_{ni}$, the transition probability of free electrons to the electron trap ($cm^3 \cdot s^{-1}$); $A_{mj}$, the transition probability of free holes to the hole trap ($cm^3 \cdot s^{-1}$); $N_i$ and $M_j$ the total concentrations of electron traps and hole traps ($cm^{-3}$); $E_{ni}$ and $E_{mj}$ the activation energies of electron and hole traps (eV); $s_{ni}$ and $s_{mj}$ the frequency factors of electron and hole traps ($s^{-1}$), $\sigma_i$ the photoionisation cross-section of light-sensitive electron trap ($cm^2$); $F$, the photon flux density ($s^{-1} \cdot cm^{-2}$); $B_j$, the transition probability of free electrons to the hole trap ($cm^3 \cdot s^{-1}$); $T_0$, the initial temperature (K); $\beta$, the linear heating rate; $k_B$, the Boltzmann's constant ($8.617 \times 10^{-5}$ eV $K^{-1}$); $X$, the production rate of electron-hole pairs during irradiation (here $5 \times 10^7$ $cm^{-3}$ $s^{-1}$ corresponds to a dose rate of 1 Gy $s^{-1}$, e.g., Bailey, 2001; Pagonis et al., 2011). Levels 1–2 of the model represent two shallow competing electron traps (labelled $S_1$ and $S_2$ in Fig. 1) yielding TL peaks at ~110 and ~190 °C. Level 3 stands for the optically active electron trap giving rising to OSL signals (i.e., the main dosimetric trap yielding a TL peak at ~325 °C, labelled M in Fig. 1). Level 4 represents a deeper competing electron trap (labelled D) yielding a TL peak at ~380 °C. Levels 5 and 6 represent the thermally unstable non-radiative recombination centre (the reservoir, labelled R) and the luminescence centre (labelled L), respectively. It is assumed that photoexcitation of electrons from levels 2 and 4 is not allowed. By taking thermal quenching of luminescence signals into account (e.g., Wintle, 1975), the OSL intensity due to recombination of electrons and holes in the L centre can be written as (Bailey, 2001):

$$L = \frac{n_c B_2 m_2}{1 + 2.8 \times 10^7 \times \exp\left(\frac{-0.64}{k_B T}\right)} \tag{5}$$

The simulation was implemented by solving the sets of differential

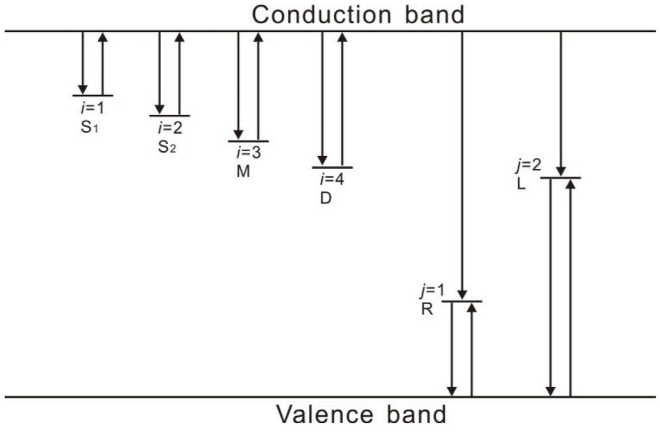


**Fig. 1.** Schematic diagram of the kinetic model used in this study.

equations with a modified KMS program (Peng and Pagonis, 2016) in the R software environment (R Core Team, 2019). The steps used for simulating the thermal and radiation history of a natural quartz sample were similar to those employed by Bailey (2001). In step 1, all trap and hole populations are set to zero for quartz crystallisation. Step 2 irradiates the sample with a 1000 Gy geological dose at 20 °C with a dose rate of 1 Gy $s^{-1}$. In step 3, the sample is heated to 350 °C to simulate the effect of geological time. Step 4 exposes the sample to OSL stimulation for 100 s at 200 °C to simulate repeated daylight exposure cycles over a long period. In step 5, the sample is irradiated with a burial dose (170 Gy) at 20 °C with a very low natural dose rate of $3.17 \times 10^{-11}$ Gy $s^{-1}$.

The achievement of a very good match between simulated and experimentally measured OSL data is not an easy task because the rate equations of charge transport in the numerical model contain a large number of parameters that need to be optimised (e.g., Adamiec et al., 2004; 2006; Weinstein and Popko, 2007). We applied the Nelder-Mead algorithm (implemented using the internal R function optim) to find out the optimal parameter set that minimises the difference between the simulated and experimentally measured data (e.g., Peng and Wang, 2020), since this algorithm works reasonably well for non-differentiable functions. The best sets of kinetic parameters were obtained using a trial-and-error protocol with different sets of initial values. The kinetic parameters required for optimisation are the electron/hole trap concentration, trapping probability, and photoionisation cross-sections of light-sensitive electron traps. The activation energy and frequency factor of each electron/hole trap were fixed during the optimisation (their values were broadly consistent with those of Bailey, 2001, 2004).

## 3. The experimental results of Choi et al. (2003a)

### 3.1. Normalised sensitivity-corrected OSL signals as a function of cycle numbers

Choi et al. (2003a) investigated the variation of normalised sensitivity-corrected OSL signals with the cycle number at different preheating conditions using quartz extracted from two poorly sorted (PNA and PYN) and two well sorted (WYN and WKR-5B) marine terrace sedimentary samples, according to the protocol of Table 1. These samples were collected from different sites. The poorly sorted sediments contain undulating or interleaved gravels and/or pebble bands separated by thin sand layers containing gravels while the well sorted sediments consist of a relatively thick layer containing sand with grain size smaller than 1 mm (Choi et al., 2003a), suggesting that the two types of sediments may originate from different sources. The two types of samples demonstrate different patterns in variations of OSL signals with measurement cycles and variations of $D_e$ determined from a dose recovery test with preheat conditions (see below).

Aliquots were bleached at room temperature with blue LEDs for 1000s, stored for 10,000 s, and bleached again for 1000 s (Steps 1–3 of Table 1). The stimulation wavelength was 470 ± 30 nm and the power density was ca. 40 mW $cm^{-2}$, yielding a photon flux density of $F = 9.452 \times 10^{16}$ $s^{-1}$ $cm^{-2}$. The PH temperature was fixed at 260 °C, and the CH temperatures were 160 °C and 220 °C. OSL stimulation was performed at 125 °C for 40 s. The regenerative and test doses were $D_r = 100$ Gy and $D_t = 10$ Gy, respectively, and the laboratory dose rate was 0.11 Gy $s^{-1}$ (see Choi et al., 2003a for details). For poorly sorted samples, a CH temperature of 160 °C resulted in an increase of normalised sensitivity-corrected OSL signals with measurement cycles while a CH temperature of 220 °C yielded a minor difference in signals between various cycles (Fig. 2a). For well sorted samples, the normalised sensitivity-corrected OSL signals in different cycle numbers were close to unity at both CH temperatures (Fig. 2b).

**Table 1**
Measurement procedures used in Choi et al. (2003a).

| Step | Description |
|---|---|
| 1 | Bleach at room temperature for 1000 s |
| 2 | Store at room temperature for 10,000 s |
| 3 | Bleach again at room temperature for 1000 s |
| 4 | Give regenerative dose $D_r$ Gy with a dose rate of 0.11 Gy $s^{-1}$ |
| 5 | Preheat at PH °C for 10 s |
| 6 | OSL stimulation at 125 °C for 40 s (obtain $L_r$) |
| 7 | Give test dose $D_t = 10$ Gy with a dose rate of 0.11 Gy $s^{-1}$ |
| 8 | Heat to CH °C for 0 s (followed by immediate cooling) |
| 9 | OSL stimulation at 125 °C for 40 s (obtain $L_t$) |
| 10 | Repeat steps 4–9 for the number of cycles ($i = 1, 2, 3, \ldots$) |

### 3.2. Dependence of the recovered $D_e$ on the preheat conditions

Choi et al. (2003a) investigated the dependence of $D_e$ determined from a dose recovery test on preheating conditions using the procedure

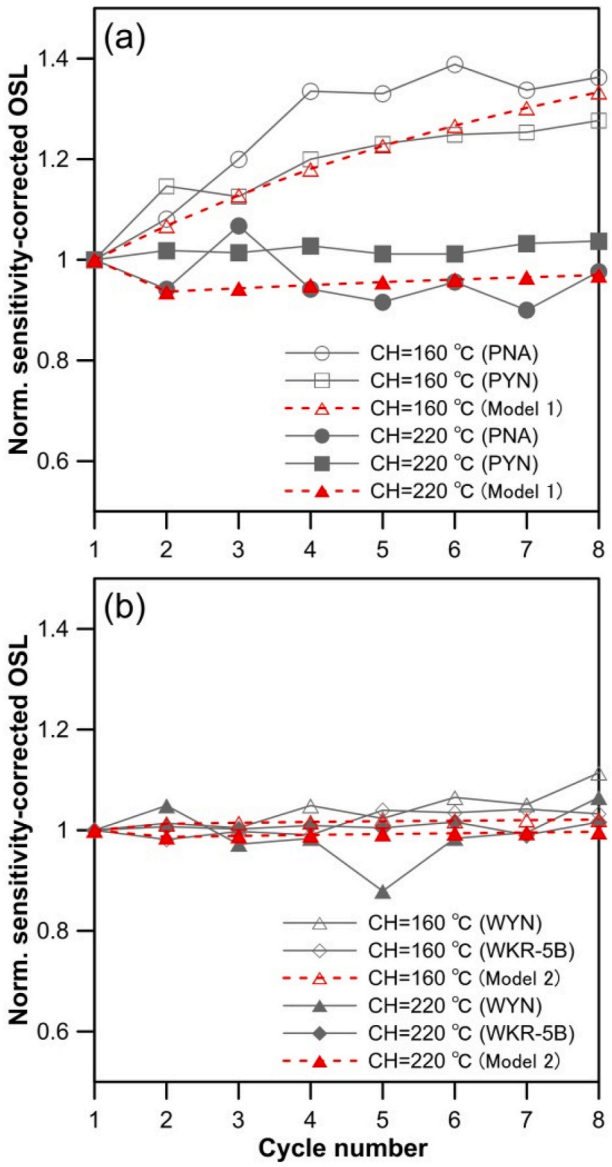


**Fig. 2.** Measured and simulated normalised sensitivity-corrected OSL signals as a function of measurement cycles, for different CH temperatures (the PH temperature was 260 °C). (a) Shows results for poorly sorted samples (PNA and PYN) and (b) shows results for well sorted samples (WYN and WKR-5B). Measured data were redrawn from Choi et al. (2003a). Simulated data for models 1 and 2 were generated using kinetic parameters of Tables 2 and 3, respectively.

of Table 1. In the first experiment, the PH temperature varied from 180 to 300 °C with a step of 20 °C and the CH temperature was fixed at 160 °C. In the second experiment, the PH temperature was fixed at 260 °C, and the CH temperature varied from 160 to 260 °C with a step of 20 °C. The dose recovery test was performed using the SAR protocol with six measurement cycles: the first cycle measured the sensitivity-corrected "natural" OSL signals, and the remaining five cycles measured the sensitivity-corrected regenerative OSL signals. The five regenerative doses were $D_{r1} = 100$ Gy, $D_{r2} = 200$ Gy, $D_{r3} = 300$ Gy, $D_{r4} = 0$ Gy, and $D_{r5} = 100$ Gy. The test dose was $D_t = 10$ Gy (see Choi et al., 2003a for details). For poorly sorted samples, when the CH temperature was fixed at 160 °C, the $D_e$ values determined from a dose recovery test were underestimated (Fig. 3a and b). The $D_e$ values recovered with CH temperatures of 160–200 °C were also underestimated when the PH temperature was fixed at 260 °C (Fig. 3d and e). For well sorted samples, there was no apparent bias (underestimation or overestimation) in recovered $D_e$ when PH (Fig. 4a and b) and CH (Fig. 4d and e) temperatures varied and, in most cases, the recovered $D_e$ values were close to the given ones.

## 4. Model parameter optimisation

As the experimentally measured results display different patterns between the two kinds of samples, we modelled them separately. We first simulated a natural sedimentary sample according to the method described in Section 2. Then the sample was further simulated according to the steps outlined in Table 1. The laboratory dose rate was 0.1 Gy $s^{-1}$, and the heating rate was 5 °C·$s^{-1}$. After each irradiation, a relaxation of a duration of 60 s was introduced, and after each heating step a cool down (with a cooling rate of 5 °C·$s^{-1}$) was added. Other laboratory parameters (including photon flux density, stimulation temperature, PH and CH temperatures, preheating and stimulation time, regenerative and test doses) used in the simulation were the same as those used by Choi et al. (2003a).

The finding of the best sets of kinetic parameters consists of two steps. In the first step, the kinetic parameters were optimised using the Nelder–Mead algorithm within a trial-and-error protocol (e.g., Peng and Wang, 2020) to obtain an initial fit. The quality of optimisation was assessed by comparing the difference between the experimentally measured and modelled data (Fig. 2). It deserves pointing out that here we chose to simulate the procedure used for measuring the variation of normalised sensitivity-corrected OSL signals as a function of cycle numbers (Fig. 2) rather than simulate the procedure used for measuring the variation of $D_e$ determined from a dose recovery test on PH/CH temperatures (Figs. 3 and 4) because the latter is much more complicated and time-consuming compared to the former.

In the second step, we manually modified the kinetic parameters obtained from step 1 by taking into account the experimentally measured dose recovery test results of Figs. 3 and 4, in order to find a best set of kinetic parameters yielding simulation results generally

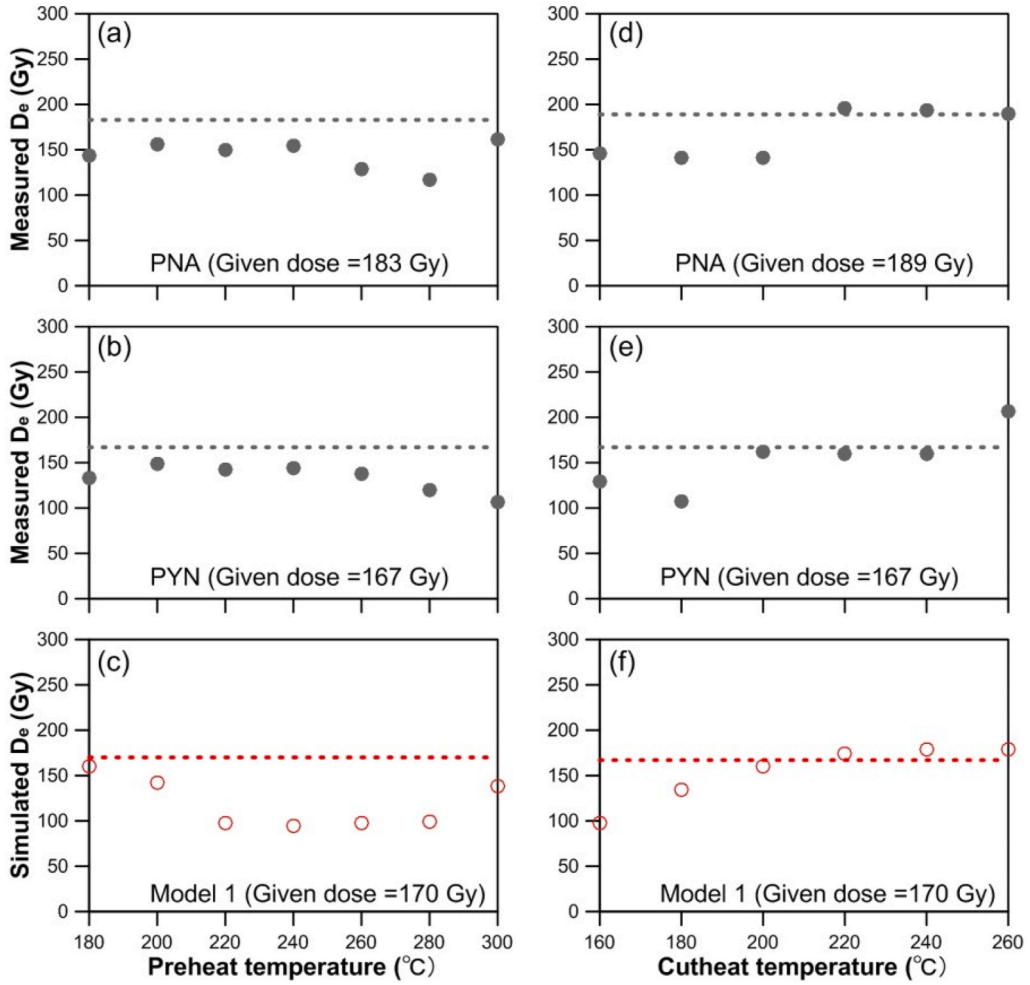


**Fig. 3.** Dependence of $D_e$ determined from a dose recovery test on PH and CH temperatures, for poorly sorted samples (PNA and PYN) and model 1 simulated using kinetic parameters of Table 2. Measured data were redrawn from Choi et al. (2003a). The dashed line indicates the given dose. In (a)–(c) the CH temperature was fixed at 160 °C while in (d)–(f) the PH temperature was fixed at 260 °C.

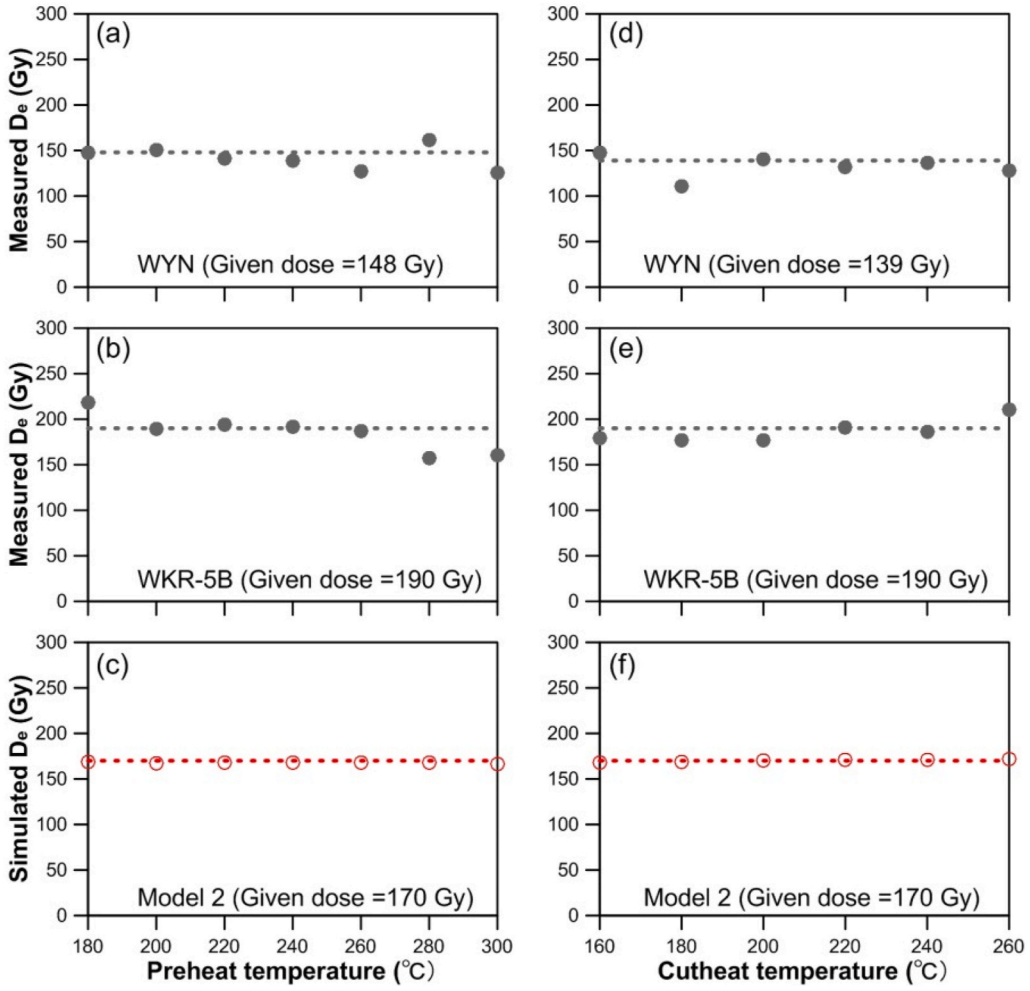


**Fig. 4.** Dependence of $D_e$ determined from a dose recovery test on PH and CH temperatures, for well sorted samples (WYN and WKR-5B) and model 2 simulated using kinetic parameters of Table 3. Measured data were redrawn from Choi et al. (2003a). The dashed line indicates the given dose. In (a)–(c) the CH temperature was fixed at 160 °C while in (d)–(f) the PH temperature was fixed at 260 °C.

consistent with both the experimental results of Sections 3.1 and 3.2. The laboratory parameters we used during the simulation of the dose recovery test were consistent with those of Choi et al. (2003a). One exception is that the administrated "natural" doses in Choi et al. (2003a) were variable (see Figs. 3 and 4) but here we selected to use a common "natural" dose of 170 Gy (treated as an unknown). The dose-response curve fitting and $D_e$ calculation were performed using the R package "numOSL" (Peng et al., 2013; Peng and Li, 2017).

The best sets of kinetic parameters are summarised in Tables 2 and 3, respectively, for poorly and well sorted samples. It can be seen from Figs. 2–4 that the simulation results obtained using the best sets of kinetic parameters are broadly consistent with the measured ones. It can be that the $N_2$ and $A_{n2}$ values (i.e., the electron trap concentration and the electron trapping probability of the $S_2$ trap) and the $M_1$ and $A_{M1}$ values (i.e., the hole trap concentration and the hole trapping probability of the R centre) in Table 2 are larger than those in Table 3. Most importantly, the ratio of electron trap concentration ($N_2/N_1$) and the ratio of electron trapping probability ($A_{N2}/A_{N1}$) between the $S_2$ and $S_1$ traps and the ratio of hole trap concentration ($M_1/M_2$) and the ratio of hole trapping probability ($A_{M1}/A_{M2}$) between the R and L centres in Table 2 are obviously larger than those in Table 3. These suggest that the influences of the $S_2$ trap and the R centre on the system is larger in model 1 compared to model 2.

**Table 2**
Optimised kinetic parameters (model 1) used for simulating the results of Fig. 2a and Fig. 3c and f. Parameters in bold are fixed during the optimisation using the Nelder-Mead algorithm.

| Level | Trap concentration ($cm^{-3}$) | Activation energy (eV) | Frequency factor ($s^{-1}$) | Trapping probability ($cm^3 \cdot s^{-1}$) | Photoionisation cross section ($cm^2$) |
|---|---|---|---|---|---|
| 1 ($S_1$) | $N_1 = 5.329 \times 10^8$ | $\mathbf{E_{n1} = 0.97}$ | $\mathbf{s_{n1} = 5 \times 10^{12}}$ | $A_{n1} = 2.013 \times 10^{-8}$ | $\sigma_1 = 6.162 \times 10^{-19}$ |
| 2 ($S_2$) | $N_2 = 6.225 \times 10^8$ | $\mathbf{E_{n2} = 1.4}$ | $\mathbf{s_{n2} = 5 \times 10^{14}}$ | $A_{n2} = 2.836 \times 10^{-8}$ | $\sigma_2 = 0$ |
| 3 (M) | $N_3 = 2.343 \times 10^{10}$ | $\mathbf{E_{n3} = 1.7}$ | $\mathbf{s_{n3} = 5 \times 10^{13}}$ | $A_{n3} = 3.738 \times 10^{-12}$ | $\sigma_3 = 1.839 \times 10^{-17}$ |
| 4 (D) | $N_4 = 5.784 \times 10^{10}$ | $\mathbf{E_{n4} = 1.8}$ | $\mathbf{s_{n4} = 2 \times 10^{13}}$ | $A_{n4} = 2.516 \times 10^{-12}$ | $\sigma_4 = 0$ |
| 5 (R) | $M_1 = 1.541 \times 10^{10}$ | $\mathbf{E_{m1} = 1.5}$ | $\mathbf{s_{m1} = 5 \times 10^{13}}$ | $A_{m1} = 7.235 \times 10^{-10}$ | – |
| | | | | $B_1 = 1.711 \times 10^{-10}$ | – |
| 6 (L) | $M_2 = 2.986 \times 10^{11}$ | $\mathbf{E_{m2} = 5.0}$ | $\mathbf{s_{m2} = 1 \times 10^{13}}$ | $A_{m2} = 6.385 \times 10^{-11}$ | – |
| | | | | $B_2 = 2.638 \times 10^{-10}$ | – |

**Table 3**
Optimised kinetic parameters (model 2) used for simulating the results of Fig. 2b and Fig. 4c and f. Parameters in bold are fixed during the optimisation using the Nelder-Mead algorithm.

| Level | Trap concentration ($cm^{-3}$) | Activation energy (eV) | Frequency factor ($s^{-1}$) | Trapping probability ($cm^3 \cdot s^{-1}$) | Photoionisation cross section ($cm^2$) |
|---|---|---|---|---|---|
| 1 ($S_1$) | $N_1 = 5.212 \times 10^8$ | $\mathbf{E_{n1} = 0.97}$ | $\mathbf{s_{n1} = 5 \times 10^{12}}$ | $A_{n1} = 1.913 \times 10^{-8}$ | $\sigma_1 = 6.511 \times 10^{-19}$ |
| 2 ($S_2$) | $N_2 = 2.026 \times 10^8$ | $\mathbf{E_{n2} = 1.4}$ | $\mathbf{s_{n2} = 5 \times 10^{14}}$ | $A_{n2} = 7.976 \times 10^{-9}$ | $\sigma_2 = 0$ |
| 3 (M) | $N_3 = 1.142 \times 10^{10}$ | $\mathbf{E_{n3} = 1.7}$ | $\mathbf{s_{n3} = 5 \times 10^{13}}$ | $A_{n3} = 6.170 \times 10^{-12}$ | $\sigma_3 = 2.215 \times 10^{-17}$ |
| 4 (D) | $N_4 = 9.706 \times 10^{10}$ | $\mathbf{E_{n4} = 1.8}$ | $\mathbf{s_{n4} = 2 \times 10^{13}}$ | $A_{n4} = 5.629 \times 10^{-12}$ | $\sigma_4 = 0$ |
| 5 (R) | $M_1 = 8.241 \times 10^9$ | $\mathbf{E_{m1} = 1.5}$ | $\mathbf{s_{m1} = 5 \times 10^{13}}$ | $A_{m1} = 3.250 \times 10^{-11}$ | – |
| | | | | $B_1 = 1.072 \times 10^{-10}$ | – |
| 6 (L) | $M_2 = 7.088 \times 10^{11}$ | $\mathbf{E_{m2} = 5.0}$ | $\mathbf{s_{m2} = 1 \times 10^{13}}$ | $A_{m2} = 1.046 \times 10^{-10}$ | – |
| | | | | $B_2 = 1.663 \times 10^{-10}$ | – |

## 5. The influence of model parameters on $D_e$ determined from a dose recovery test

The following six effects involved during preheating may affect the OSL intensity and the results of the SAR protocol, and their influence can change with the PH/CH temperatures:

(1) The second shallow electron ($S_2$) trap yields a TL peak at ~190 °C. Heating at higher temperatures excites more electrons from the $S_2$ trap into recombination centres and therefore consumes more holes. As a consequence, fewer holes are available in the luminescence (L) centre to recombine with electrons excited from the main electron (M) trap in the subsequent stimulation stage. This effect will be significant if electron trapping probabilities of the recombination centres are large (i.e., if recombination dominates). This kind of thermal desensitisation may lead to a continuous decrease in subsequent OSL intensity as the $S_2$ trap is increasingly thermally emptied at higher PH/CH temperatures. Note that this effect is different from the optical desensitisation occurring during stimulation (Bailey, 2001).

(2) The concentration of electrons trapped in the $S_2$ trap increases with the decrease of PH/CH temperatures. Subsequently, these trapped electrons are thermally excited into recombination centres (if recombination dominates) during OSL stimulation. As a consequence, a low PH/CH temperature prompts the increase of subsequent OSL intensity. This is responsible for the presence of phosphorescence signals in subsequently measured OSL if prior PH/CH temperature is low (Choi et al., 2003b; Jacobs et al., 2006b). It deserves pointing out that for the 190 °C TL peak contained in our model the thermal excitation is insignificant if OSL stimulation is performed at 125 °C for 40 s. However, the effect of thermal excitation during OSL stimulation cannot be neglected if the peak temperature of the trap is lower (such as 160 °C or 175 °C) or if the stimulation temperature is higher. Considered that we include a 190 °C TL peak to conceptually represent TL peaks originated from shallow electron traps other than the 110 °C TL peak (in the temperature range of 130–300 °C) that are widely reported in natural quartz samples, Mechanism 2 will be significant for TL peaks with peak temperature lower than 190 °C. In addition, optical excitation of electrons into recombination centres during stimulation is also possible (although in our model the $S_2$ trap is optically insensitive), if a shallow trap is optically sensitive and has a larger optical cross-section (e.g., Choi et al., 2003a).

(3) If the electron trapping probability coefficient of the $S_2$ trap is large, then electrons excited from the M trap during optical stimulation are likely to accumulate in the $S_2$ trap (when the stimulation temperature is lower than 190 °C). The number of phototransferred electrons gained in the $S_2$ trap during subsequent stimulation increases with prior PH/CH temperatures, since higher PH/CH temperatures prompt the thermal bleaching of the $S_2$ trap. This gives rise to the decrease of subsequent OSL intensity with increased PH/CH temperatures. Phototransfer during stimulation is widely observed in shallow traps of quartz (e.g., Bailiff et al., 1977; Wang et al., 2015; Peng and Wang, 2020).

(4) As the sample temperature is approaching the peak temperature of a TL glow peak, more electrons are excited from the trap due to thermal eviction (Aitken, 1985). Accordingly, fewer electrons are available in the M trap to recombine with holes in the L centre in the subsequent stimulation stage. The M trap yields a TL peak at ~325 °C. This leads to a substantial decrease of the OSL intensity as PH/CH temperatures approach 325 °C.

(5) If recombination dominates, the favourable direction for electrons is from the M trap to the L centre during heating (through thermal excitation) when the PH/CH temperature is ≥ 300 °C. The number of electrons that recombine in the R centre is negligible during heating when the PH/CH temperature exceeds 300 °C, since in our model the reservoir is highly thermally unstable at 300 °C ($E_{m1} = 1.5$ eV, $s_{m1} = 5 \times 10^{13}$ $s^{-1}$, see Tables 2 and 3). In contrast, at lower PH/CH temperatures, number of electrons that are captured by the L centre will be smaller during heating, because the R centre also competes for free electrons excited from the M trap in this case. In consequence, OSL intensities measured following a PH/CH temperature of ≥300 °C are significantly lower.

(6) The R centre is thermally unstable and releases holes in the valence band at a peak temperature of ~260 °C. As the PH/CH temperature approaches 260 °C, more holes are transferred from the R centre into the L centre as a result of thermal activation (e.g., Zimmerman, 1971). This leads to a continuous increase of OSL intensity as holes in the R centre are increasingly excited at higher PH/CH temperatures. This effect will be significant for laboratory irradiated samples (e.g., Wintle and Murray, 1998; Wang et al., 2021) and is expected to be controlled by the hole trap concentration and hole trapping probability of the R centre (Pagonis et al., 2007).

We present the natural/regenerative OSL intensities as well as their test dose OSL intensities as a function of SAR cycles (Figs. 5 and 6) to reveal the potential mechanism responsible for the underestimation of recovered $D_e$. The "natural" and regenerative OSL intensities correspond to the 1st and the 2nd–6th SAR cycles, respectively.

### 5.1. The first model

The electron trapping probability coefficients for the M, D, R, and L competitors are $A_{n3} = 3.74 \times 10^{-12}$, $A_{n4} = 2.52 \times 10^{-12}$, $B_1 = 1.71 \times 10^{-10}$, and $B_2 = 2.64 \times 10^{-10}$ $cm^3$ $s^{-1}$, respectively (see Table 2). As a consequence, $mB_2$ will be significantly larger than $(N_3\text{-}n_3)A_{n3}$ and $(N_4\text{-}n_4)A_{n4}$ (in Eqs. (1) and (2)), suggesting that the competition for free electrons in the L centre will be significantly larger than that in the M and D competitors (i.e., recombination dominates and therefore favouring effects 1, 2, and 5). The electron trapping probability coefficient of the $S_2$ trap (i.e., $A_{n2} = 2.84 \times 10^{-8}$ $cm^3$ $s^{-1}$) is the largest, favouring effect 3. Although the hole trap concentration of the R centre

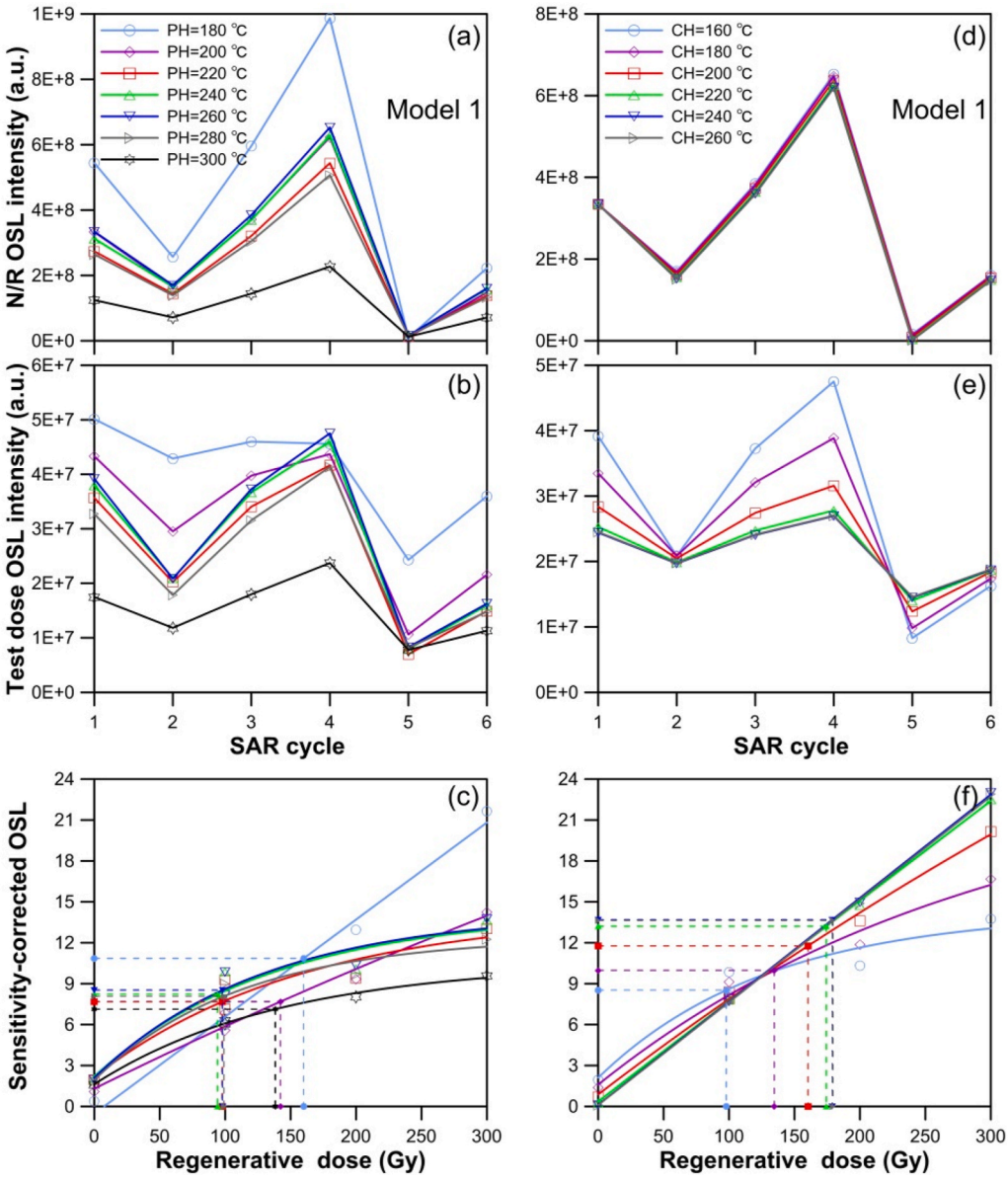


**Fig. 5.** Natural/regenerative (a) and test dose (b) OSL intensities as a function of SAR cycles, for various PH temperatures. (c) $D_e$ determination using sensitivity-corrected OSL signals, for various PH temperatures. Cycle 1 corresponds to the "natural" dose of 170 Gy, Cycles 2–6 corresponds to regenerative doses of 100, 200, 300, 0, and 100 Gy, respectively. Legends in (b) and (c) are the same as (a). (d)–(f) are the same as (a)–(c), but for various CH temperatures. These results were simulated using kinetic parameters of Table 2 for model 1. Note that in (a)–(c) the CH temperature was fixed at 160 °C while in (d)–(f) the PH temperature was fixed at 260 °C.

($M_1 = 1.54 \times 10^{10}$ cm$^{-3}$) is one order smaller than that of the L centre ($M_2 = 2.99 \times 10^{11}$ cm$^{-3}$), the hole trapping probability coefficient of the R centre ($A_{m1} = 7.24 \times 10^{-10}$ cm$^3$ s$^{-1}$) is one order larger than that of the L centre ($A_{m2} = 6.39 \times 10^{-11}$ cm$^3$ s$^{-1}$), favouring effect 6. The natural/regenerative OSL intensities are highest at PH = 180 °C because at this temperature effects 1–3 prevail (Fig. 5a). The intensities are lowest at PH = 300 °C as a result of effects 4–5. OSL intensities at intermediate PH temperatures sorted in decreasing order are measured at PH temperatures of 260, 240, 200, 220, and 280 °C, which are controlled by complex coupling between effects 1–6.

The difference in PH temperatures used before the measurement of natural/regenerative OSL responses also exerts significant influence on the variation of subsequent test dose OSL intensities (Fig. 5b), although the CH temperature was fixed at 160 °C. Test dose OSL intensities corresponding to PH temperatures of 180 and 200 °C are the highest (except the case of cycle 4). This can be explained by the fact that the strength of thermal excitation of electrons from the $S_2$ trap is lower at lower PH temperatures (compared to higher PH temperatures) and therefore during the subsequent test dose irradiation the competition for electrons in the $S_2$ trap is weaker. In consequence, more electrons are trapped into the M trap, and the test dose OSL intensity increases in the following stimulation stage. Test dose OSL intensities at PH = 300 °C are the lowest. At PH = 300 °C more electrons thermally excited from the M trap are captured by the L centre as the competition for electrons in the R centre is negligible (i.e., effect 5). This results in substantial decreases in both regenerative and test dose OSL intensities. In addition, we noted that the variation of test dose OSL intensities between different cycles is smaller if the PH temperature is 180, 200, or 300 °C (Fig. 5b). The test dose OSL intensity increases substantially during the 2–4 cycles (corresponding to $D_r$ of 100–300 Gy) in the PH temperature range of 220–280 °C. In contrast, the increase of test dose OSL intensity during the 2–4 cycles is relatively small if the PH temperature is 180, 200, or 300 °C. Interestingly, $D_e$ underestimation is not very serious (<20%) if the PH temperature is 180, 200, or 300 °C and becomes very significant (>40%) in the PH temperature range of 220–280 °C (Fig. 5c). This is not by coincidence, but there is a direct relationship between them.

As stated above, the strength of thermal excitation of electrons from the $S_2$ trap is slightly lower at lower PH temperature (180–200 °C), and therefore the competition for electrons in the $S_2$ trap is relatively weaker during the subsequent irradiation with the test dose. This results in an

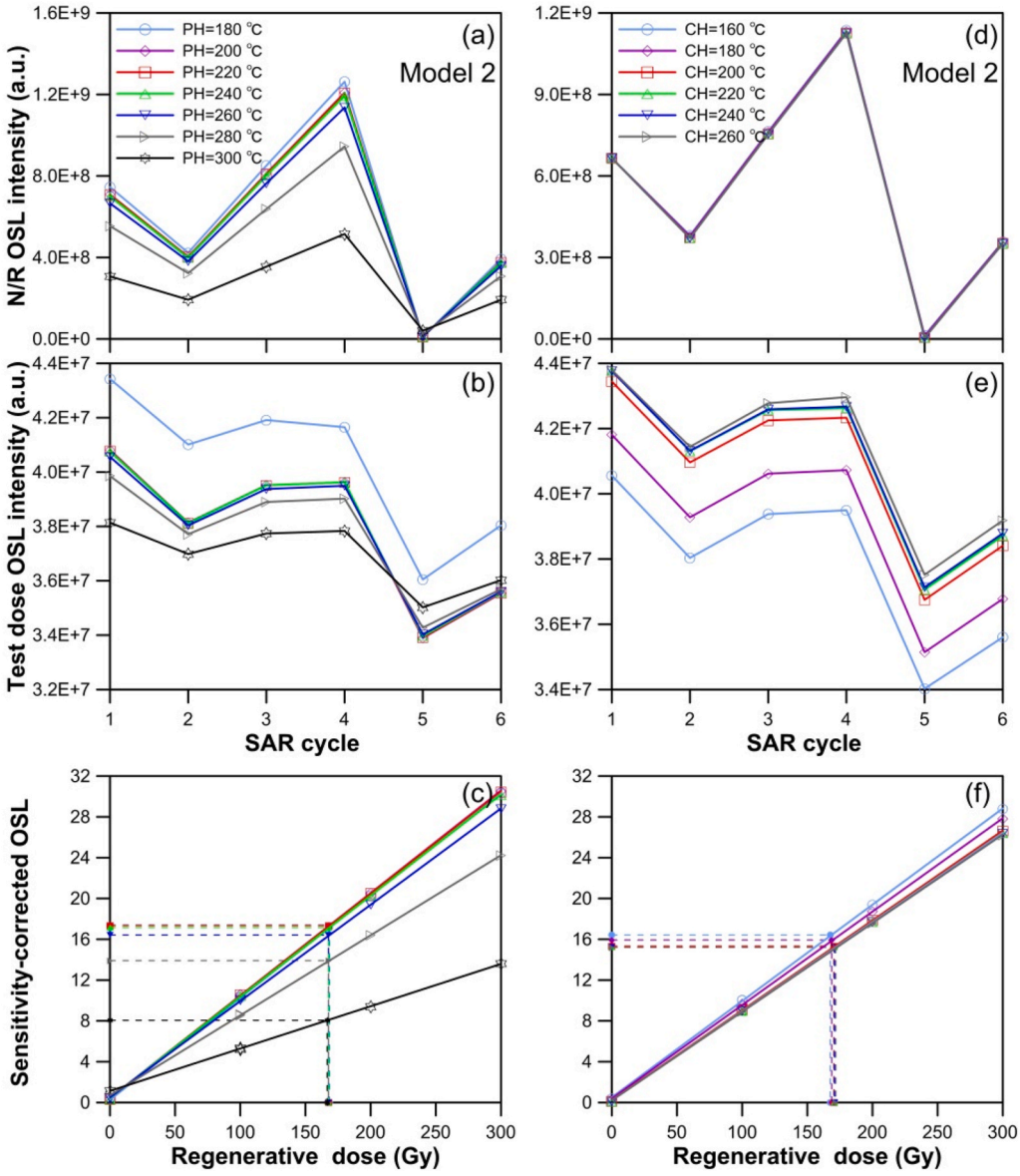


**Fig. 6.** The same as Fig. 5, but simulated using kinetic parameters of Table 3 for model 2.

increase of test dose OSL intensity in the following OSL stimulation if lower PH temperatures are used. On the contrary, at higher PH temperatures, the $S_2$ trap competes strongly for free electrons during test dose irradiation as the trap is previously fully emptied by preheating. Furthermore, the difference in test dose OSL intensities between PH temperatures of 180–280 °C is especially significant at $D_r$ = 100 Gy (cycle 2) and becomes insignificant at $D_r$ = 300 Gy (cycle 4) (Fig. 5b). The decrease in test dose OSL intensities at higher PH temperatures caused by effects 1–3 is compensated to some extent by the increase in test dose OSL intensities due to thermal activation of the R centre when $D_r$ = 300 Gy. In other words, the resultant test dose OSL intensities become increasingly dominated by effect 6 (rather than effects 1–3) when the regenerative dose increases.

In conclusion, we argue that the serious $D_e$ underestimation in the PH temperature range of 220–280 °C results from the intervention of the $S_2$ trap, which leads to significant changes in the test dose OSL intensity with regenerative dose (when CH = 160 °C). As a result, the regenerative OSL signals cannot be successfully corrected using the test dose OSL signals. In addition, we argue that in the case of PH = 300 °C the intervention effect of the $S_2$ trap was influenced by thermal eviction of electrons from the M trap (effect 4), which is the reason why the increase of the test dose OSL intensity during the 2–4 cycles is small when PH = 300 °C.

The difference in regenerative OSL intensities corresponding to different CH temperatures is insignificant when PH temperature is fixed at 260 °C (Fig. 5d). The results of Fig. 5e are different from those of Fig. 5b, since the PH temperature is fixed at 260 °C. As a consequence, effects 4–6 may exert minor influence on the results. The test dose OSL intensity decreases when CH temperature increases (Fig. 5e), which results directly from effects 1–3, i.e., desensitisation of the L centre during preheating, decreased contribution from phosphorescence signals, and increased competition for electrons in the $S_2$ trap during stimulation. The strong decrease of the test dose OSL intensity with CH temperature caused by effects 1–3 cannot be compensated by the increase of the test dose OSL intensity due to thermal sensitisation of the L centre (effect 6), because the test dose used is small (10 Gy).

$D_e$ underestimation becomes increasingly serious when the CH temperature decreases from 260 to 160 °C (Fig. 5f). Variation in the test dose OSL intensity across different regenerative doses is the largest and the recovered $D_e$ is most seriously underestimated if the CH temperature

is 160 °C. By contrast, a CH temperature of 260 °C yields the smallest variation of test dose OSL intensity and the most accurate $D_e$ estimate. This demonstrates that the unwanted effects of the $S_2$ trap on $D_e$ determination will be significant if the difference between PH and CH temperature is large.

### 5.2. The second model

Here, the electron trapping probability coefficients for the M, D, R, and L competitors are $A_{n3} = 6.17 \times 10^{-12}$, $A_{n4} = 5.63 \times 10^{-12}$, $B_1 = 1.07 \times 10^{-10}$, and $B_2 = 1.66 \times 10^{-10}$ $cm^3\ s^{-1}$ (Table 3), favouring effects 1, 2, and 5. The electron trapping probability coefficient of the $S_2$ trap (i.e., $A_{n2} = 7.98 \times 10^{-9}$ $cm^3\ s^{-1}$) is larger than that of M, D, R, or L, favouring effect 3. The hole trap concentration of the R centre ($M_1 = 8.24 \times 10^9$ $cm^{-3}$) is two orders smaller than that of the L centre ($M_2 = 7.09 \times 10^{11}$ $cm^{-3}$), and the hole trapping probability coefficient of the R centre ($A_{m1} = 3.25 \times 10^{-11}$ $cm^3\ s^{-1}$) is one order smaller than that of the L centre ($A_{m2} = 1.05 \times 10^{-10}$ $cm^3\ s^{-1}$), suggesting effect 6 is insignificant. The regenerative OSL intensity decreases monotonically with PH temperatures (Fig. 6a). However, we note that the results of Fig. 6a are very different from those of Fig. 5a. This is because both the electron trap concentration and trapping probability of the $S_2$ trap are smaller and therefore the influence of effects 1–3 is smaller, and both the hole trap concentration and trapping probability of the R centre are smaller, and therefore the influence of effect 6 is smaller in the second model. For the same reasons, we observe that the results of Fig. 6b are very different from those of Fig. 5b. The test dose OSL intensities at PH temperature range of 220–280 °C in Fig. 6b are less variable compared to those in Fig. 5b. As a result, the dose response curves are less scattered, and the given doses are accurately recovered (Fig. 6c). Interestingly, the variation pattern of dose response curves with PH temperatures seen in Fig. 6c is broadly consistent with that of Roberts and Duller (2004), for a coarse-grained quartz sample (TNE9513) measured using the same CH temperature (i.e., 160 °C).

The results of Fig. 6d are similar to those of Fig. 5d. In Fig. 6e, however, the test dose OSL intensity increases when CH temperature increases, which is significantly different from that in Fig. 5e. This is attributed to the fact that the decrease of test dose OSL intensity with CH temperatures caused by effects 1–3 was compensated by the increase of the test dose OSL intensity due to thermal sensitisation of the L centre (effect 6) since the influence of effects 1–3 was much smaller (although effect 6 was also smaller) in the second model. In addition, in Fig. 6e, the variations in test dose OSL intensities across different regenerative doses are smaller compared to those seen in Fig. 5e. The dose response curves are less scattered, and the given doses are accurately recovered (Fig. 6f).

### 5.3. Simulation of the influence of the shallow electron trap

In this section, we further illustrate the difference between models 1 and 2, and show how the parameters in the models can influence their respective results. For this purpose, we simulated the variation of normalised sensitivity-corrected OSL signals as a function of cycle numbers

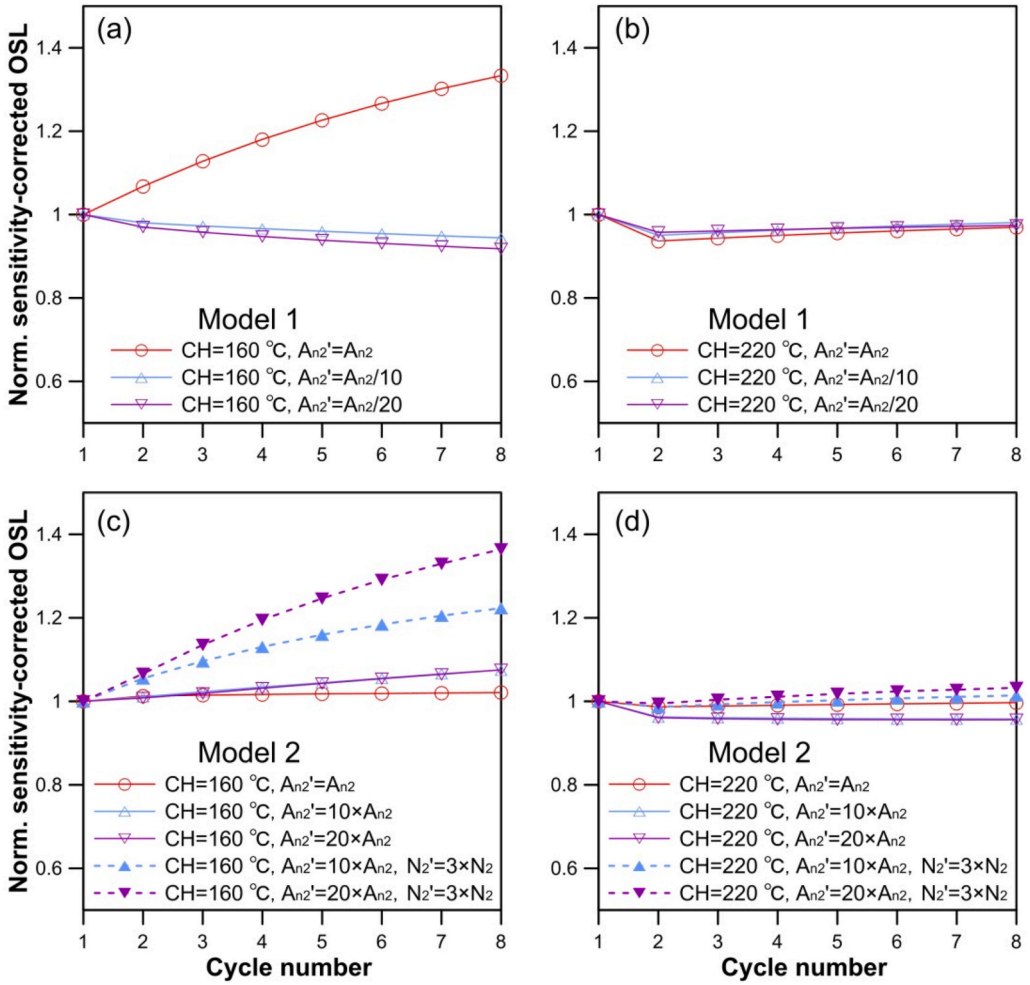


**Fig. 7.** Normalised sensitivity-corrected OSL signals as a function of measurement cycles, for various CH temperatures and kinetic parameters. The PH temperature was fixed at 260 °C. (a)–(b) and (c)–(d) were simulated using kinetic parameters of Tables 2 and 3, respectively.

using the same procedure as Section 3.1, and simulated the dependence of recovered $D_e$ on preheating conditions using the same procedure as Section 3.2, but changed the competition parameters for electrons in the $S_2$ trap. The results are presented in Figs. 7–10.

**Model 1**. The electron trapping probability coefficient of the $S_2$ trap ($A_{n2}$) was changed to be one-tenth and one-twentieth of the original value. In the case of CH = 160 °C, the normalised sensitivity-corrected OSL signals decrease slightly with the measurement cycles and are very close to unity as $A_{n2}$ decreases (Fig. 7a) (the results are very similar to Fig. 2b). In the case of CH = 220 °C, the normalised sensitivity-corrected OSL signals are insensitive to the decrease of $A_{n2}$ (Fig. 7b). The given dose can be recovered very accurately as $A_{n2}$ decreases (Fig. 8a and b). The recycling ratios (Fig. 9a and b) and recuperation values (Fig. 10a and b) are also decreased dramatically as $A_{n2}$ decreases. We were able to reproduce the results of model 2 by decreasing the trapping ability of the $S_2$ trap.

**Model 2**. The normalised sensitivity-corrected OSL signals increased slightly in the case of CH = 160 °C when $A_{n2}$ was changed to be 10 or 20 times of the original value (Fig. 7c). If we further changed the electron trap concentration of the $S_2$ trap ($N_2$) to be three times of the original value, the normalised sensitivity-corrected OSL signals increase substantially (the results are similar to Fig. 2a). In the case of CH = 220 °C, the normalised sensitivity-corrected OSL signals are insensitive to the decrease of $A_{n2}$ and/or $N_2$ (Fig. 7d). The given dose becomes increasingly underestimated as $A_{n2}$ and/or $N_2$ increases (Fig. 8c and d). The recycling ratios (Fig. 9c and d) and recuperations (Fig. 10c and d) are also amplified dramatically as $A_{n2}$ and/or $N_2$ increases. We can reproduce the results of model 1 by increase the trapping ability of the $S_2$ trap.

## 6. Discussion and conclusions

A kinetic model was used to simulate the variations of normalised sensitivity-corrected OSL signals as a function of cycle numbers and dependences of recovered $D_e$ on the preheating conditions. It demonstrates that the experimentally measured results of Choi et al. (2003a) can be successfully reproduced by a set of kinetic parameters obtained using an optimisation algorithm (Tables 2 and 3). For each trap level, the two models have the same trap depths (determined by the activation energy and frequency factor), but different trap concentrations, trapping probabilities, and photoionisation cross-sections. Elevated PH temperature prompts the excitation of electrons from the $S_2$ trap, and as a result, the trap will compete for more electrons during subsequent irradiation with test dose. This leads to apparent smaller test dose OSL intensity at higher PH temperatures (see Fig. 5b). Elevated CH temperature prompts the movement of electrons from the $S_2$ trap into the recombination centre (if recombination dominates), and as a result, the hole concentration in the L centre will have decreased during subsequent stimulation. In consequence, the test dose OSL intensity is smaller at higher CH temperatures (see Fig. 5e). The results of Fig. 5b and e suggest that test dose OSL intensities vary more significantly among different regenerative doses if the difference between PH and CH temperatures is larger. It demonstrates that the regenerative OSL signals cannot be properly corrected if the test dose OSL intensity varies

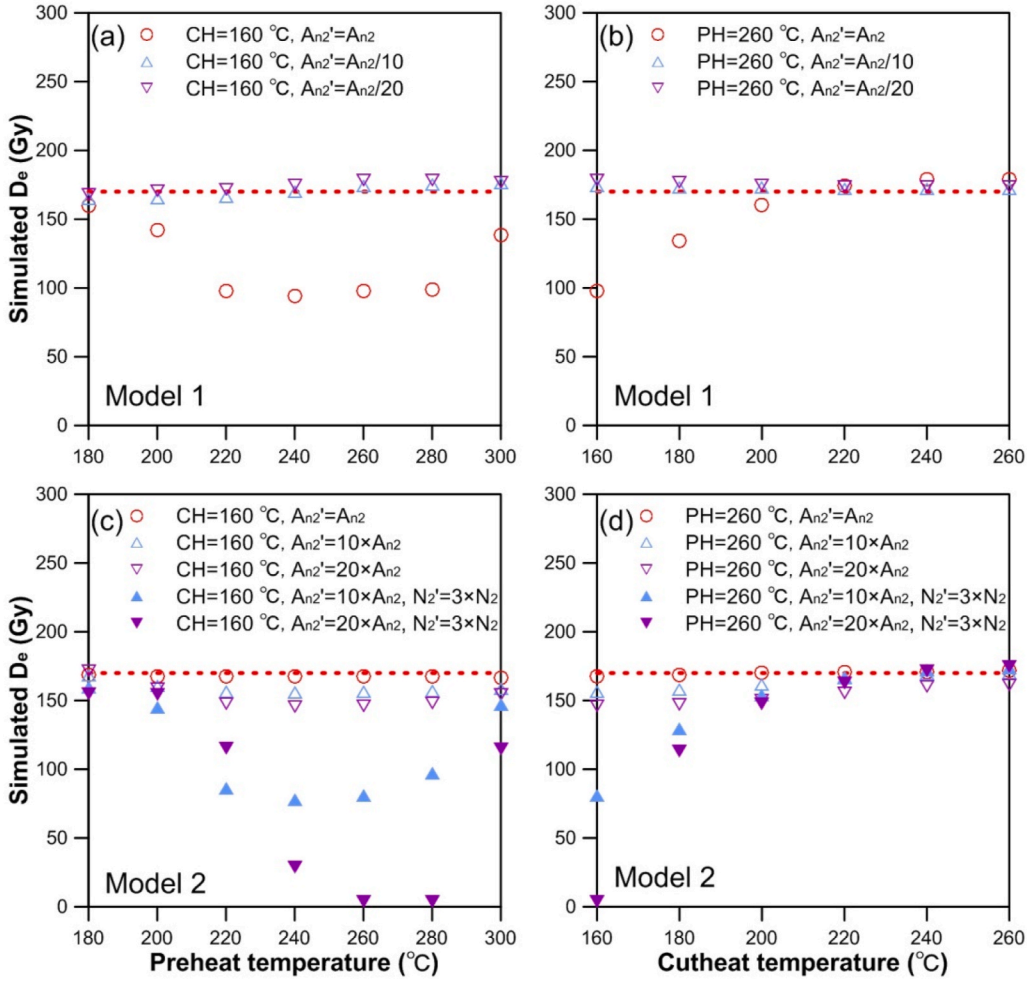


**Fig. 8.** Recovered $D_e$ as a function of PH and CH temperatures, for various kinetic parameters. (a)–(b) and (c)–(d) were simulated using kinetic parameters of Tables 2 and 3, respectively. The dashed line indicates the given dose.

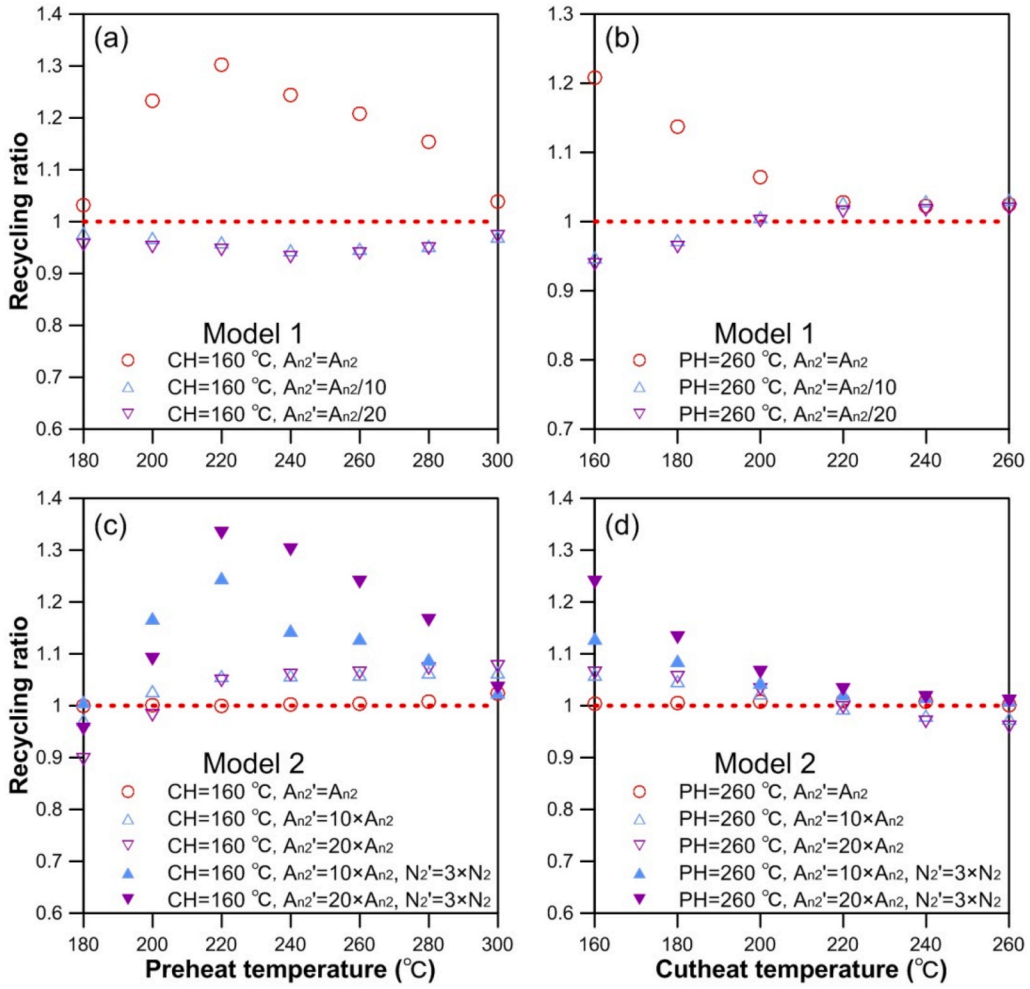


**Fig. 9.** Recycling ratios as a function of PH and CH temperatures, for various kinetic parameters. (a)–(b) and (c)–(d) were simulated using kinetic parameters of Tables 2 and 3, respectively. The dashed line indicates a perfect recycling ratio of unity.

significantly (see Fig. 5c and f), leading to more underestimation of recovered $D_e$ (Fig. 8a and b), poor recycling ratio (Fig. 9a and b), and large recuperation (Fig. 10a and b).

However, we demonstrated that a larger difference between PH and CH temperature is only a necessary condition (not a sufficient condition) for significant underestimation of recovered $D_e$, since in the second model the dose recovery test shows good performance, even if the PH temperature is higher and the CH temperature is lower (see Figs. 6, Fig. 8c and d, Fig. 9c and d, and Fig. 10c and d). This originates from the fact that the trapping ability of the $S_2$ trap in the second model is smaller than that in the first model. The first model resembles the second one, if the trapping ability of the $S_2$ trap decreases, and vice versa (see Figs. 7–10). The simulation results explain why the results of a dose recovery experiment for some sedimentary samples are more sensitive to the preheating conditions compared to others (e.g., Choi et al., 2003a; Jacobs et al., 2006b). It also reveals why a higher CH temperature performs better for some samples. Choi et al. (2003a, b) proposed to use a CH temperature of 220 °C for their quartz samples. Murray and Wintle (2003) suggested using a CH temperature that was 20 °C lower than the PH temperature in the construction of plots of $D_e$ as a function of PH temperature. Jacobs et al. (2006b) suggested using a CH temperature only ~20–40 °C below the PH temperature. Our simulation results imply that to resolve the side-effects of shallow electron traps, it is best to use a CH temperature equal to (or very close to) the PH temperature during the application of the SAR protocol. Equal PH and CH temperatures have been adopted in OSL dating of quartz samples extracted from Chinese loess (e.g., 260 °C in Chapot et al., 2012; 230 °C in Wang et al., 2021).

Wintle and Murray (2006) pointed out that a lower CH temperature such as 160 °C suggested by Murray and Wintle (2000) may be inappropriate, if in some samples there are shallow traps (like the ones responsible for the ultrafast component), in which cases the test dose response does not monitor the sensitivity change correctly. Although in most cases TL peaks originating from shallow traps are of significantly lesser magnitude than those at ~110 and ~330 °C, there may exist a large number of traps of this kind between 100 and 300 °C (e.g., Aitken, 1985; Spooner and Questiaux, 2000; Pagonis et al., 2002). Also, there are samples for which the electron released from such trap is significant (Rhodes and Bailey, 1997). The simulations showed that the test dose OSL signals might fail to correct the regenerative ones, if the intervention of shallow electron traps is strong, which is in agreement with Wintle and Murray (2006). Both Choi et al. (2003b) and Jacobs et al. (2006b) observed a strong phosphorescence signal included in OSL signals in the lower preheat temperature ranges and a significant decrease of the phosphorescence signal at elevated heating temperatures. This is because the influence of the shallow traps decreases with the increase of the heating temperature.

Although the kinetic model used here represents only a simplification for describing the traffic of carriers between charge competitors in natural quartz, based on the simulation results, we argue that the underestimation of recovered $D_e$ at lower CH temperature reported previously (e.g., Choi et al., 2003a; Jacobs et al., 2006b) was at least partly attributed to the intervention of shallow electron traps. We caution

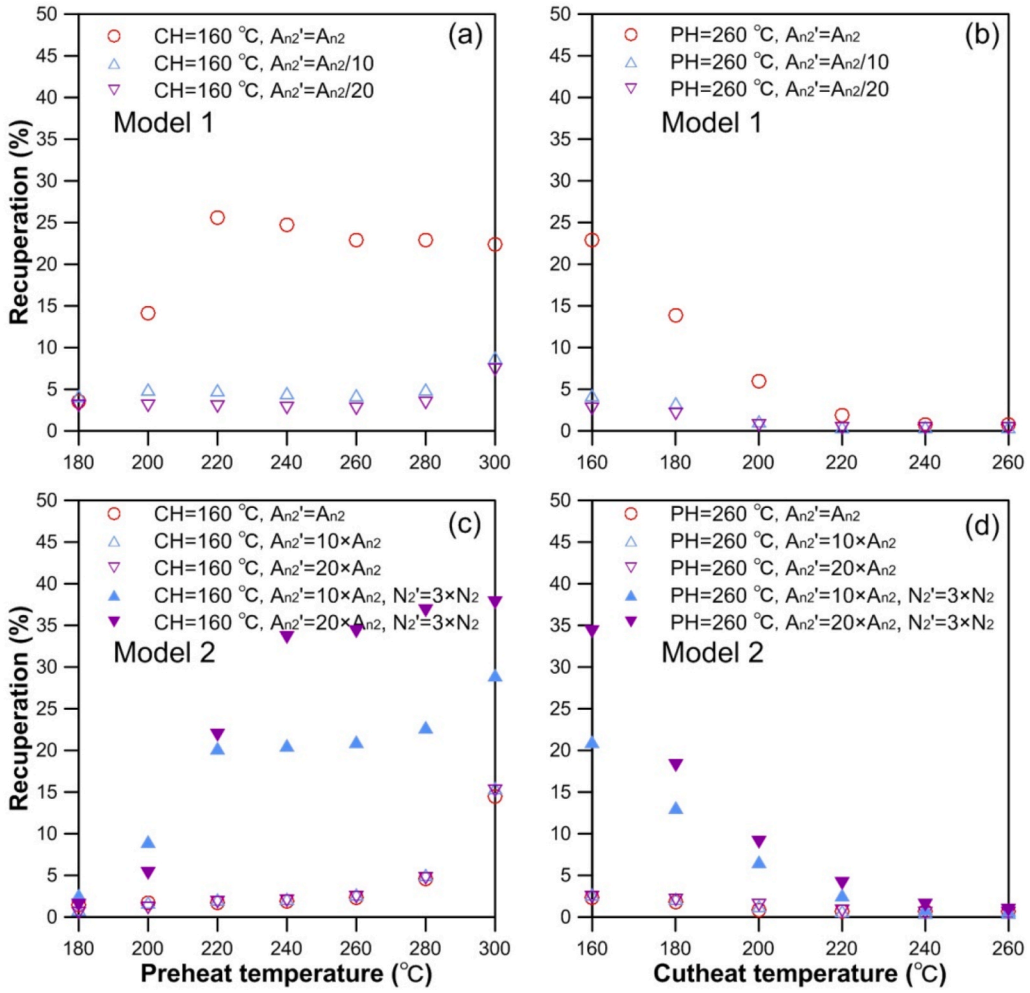


**Fig. 10.** Recuperations as a function of PH and CH temperatures, for various kinetic parameters. (a)–(b) and (c)–(d) were simulated using kinetic parameters of Tables 2 and 3, respectively.

against the use of a CH temperature that is obviously lower than the PH temperature during SAR $D_e$ determination, especially for samples containing a significant number of electrons in their shallow traps.

## Declaration of competing interest

The authors declare that they have no known competing financial interests or personal relationships that could have appeared to influence the work reported in this paper.

## Acknowledgements

We appreciate three anonymous reviewers for their comments and suggestions which improve the quality of this manuscript. This research was funded by the National Natural Science Foundation of China (Grant No. 41701004) and the Natural Science Foundation of Hunan Province, China (Grant No. 2020JJ5162) to J. Peng. X.L. Wang would like to acknowledge the SPRP of Chinese Academy of Sciences (Grant No. XDB40010100). G. Adamiec would like to acknowledge the grant of the National Science Centre, Poland (Grant No. 2016/21/B/ST10/01867). J.H. Choi was supported by the KBSI project fund (Grant No. C050100).

## References

Adamiec, G., Garcia-Talavera, M., Bailey, R.M., De La Torre, P.I., 2004. Application of a genetic algorithm to finding parameter values for numerical stimulation of quartz luminescence. Geochronometria 23, 9–14.

Adamiec, G., Bluszcz, A., Bailey, R., Garcia-Talavera, M., 2006. Finding model parameters: genetic algorithms and the numerical modelling of quartz luminescence. Radiat. Meas. 41 (7–8), 897–902.

Aitken, M.J., 1985. Thermoluminescence Dating. Academic press, London, p. 272.

Aitken, M.J., Smith, B.W., 1988. Optical dating: recuperation after bleaching. Quat. Sci. Rev. 7 (3–4), 387–393.

Ankjærgaard, C., Jain, M., 2010. Optically stimulated phosphorescence in quartz over the millisecond to second time scale: insights into the role of shallow traps in delaying luminescent recombination. J. Phys. D Appl. Phys. 43 (25), 255502.

Bailey, R.M., 2000. Circumventing possible inaccuracies of the single aliquot regeneration method for the optical dating of quartz. Radiat. Meas. 32 (5–6), 833–840.

Bailey, R.M., 2001. Towards a general kinetic model for optically and thermally stimulated luminescence of quartz. Radiat. Meas. 33 (1), 17–45.

Bailey, R.M., 2004. Paper I—simulation of dose absorption in quartz over geological timescales and its implications for the precision and accuracy of optical dating. Radiat. Meas. 38 (3), 299–310.

Bailiff, I.K., Bowman, S.G.E., Mobbs, S.F., Aitken, M.J., 1977. The phototransfer technique and its use in thermoluminescence dating. J. Electrost. 3 (1–3), 269–280.

Chapot, M.S., Roberts, H.M., Duller, G.A.T., Lai, Z.P., 2012. A comparison of natural- and laboratory-generated dose response curves for quartz optically stimulated luminescence signals from Chinese Loess. Radiat. Meas. 47 (11–12), 1045–1052.

Choi, J.H., Murray, A.S., Jain, M., Cheong, C.S., Chang, H.W., 2003a. Luminescence dating of well-sorted marine terrace sediments on the southeastern coast of Korea. Quat. Sci. Rev. 22 (2–4), 407–421.

Choi, J.H., Murray, A.S., Cheong, C.S., Hong, D.G., Chang, H.W., 2003b. The resolution of stratigraphic inconsistency in the luminescence ages of marine terrace sediments from Korea. Quat. Sci. Rev. 22 (10–13), 1201–1206.

Choi, J.H., Murray, A.S., Cheong, C.S., Hong, S.C., 2009. The dependence of dose recovery experiments on the bleaching of natural quartz OSL using different light sources. Radiat. Meas. 44, 600–605.

Chruścińska, A., Przegiętka, K.R., 2010. The influence of electron–phonon interaction on the OSL decay curve shape. Radiat. Meas. 45 (3–6), 317–319.

Chruścińska, A., Przegiętka, K.R., 2011. Analysis of OSL intensity increase with temperature and its consequences for dating applications. Radiat. Meas. 12, 1514–1517.
Duller, G.A.T., 2012. Improving the accuracy and precision of equivalent doses determined using the optically stimulated luminescence signal from single grains of quartz. Radiat. Meas. 47 (9), 770–777.
Feathers, J.K., Pagonis, V., 2015. Dating quartz near saturation - Simulations and application atarchaeological sites in South Africa and South Carolina. Quat. Geochronol. 30, 416–421.
Jacobs, Z., Duller, G.A.T., Wintle, A.G., 2006a. Interpretation of single grain De distributions and calculation of De. Radiat. Meas. 41 (3), 264–277.
Jacobs, Z., Wintle, A.G., Duller, G.A.T., 2006b. Evaluation of SAR procedures for De determination using single aliquots of quartz from two archaeological sites in South Africa. Radiat. Meas. 41 (5), 520–533.
Kijek, N., Chruścińska, A., 2015. Equivalent dose of quartz originating from ceramics obtained by OSL SAR method – tests of protocol parameters. Radiat. Meas. 81, 128–133.
Kijek, N., Chruścińska, A., Przegiętka, K.R., 2013. On the dependence of equivalent dose on temperature of OSL measurements for sediment quartz grains and its implication in dating practice. Radiat. Meas. 56, 252–256.
McKeever, S.W.S., Bøtter-Jensen, L., Larsen, N.A., Duller, G.A.T., 1997a. Temperature dependence of OSL decay curves: experimental and theoretical aspects. Radiat. Meas. 27 (2), 161–170.
McKeever, S.W.S., Larsen, N.A., Bøtter-Jensen, Mejdahl, V., 1997b. OSL sensitivity changes during single aliquot procedures: computer simulations. Radiat. Meas. 27 (2), 75–82.
Murray, A.S., Wintle, A.G., 2000. Luminescence dating of quartz using an improved single-aliquot regenerative-dose protocol. Radiat. Meas. 32 (1), 57–73.
Murray, A.S., Wintle, A.G., 2003. The single aliquot regenerative dose protocol: potential for improvements in reliability. Radiat. Meas. 37 (4–5), 377–381.
Pagonis, V., Tatsis, E., Kitis, G., Drupieski, C., 2002. Search for common characteristics in the glow curves of quartz of various origins. Radiat. Protect. Dosim. 100 (1–4), 373–376.
Pagonis, V., Wintle, A.G., Chen, R., 2007. Simulations of the effect of pulse annealing on optically-stimulated luminescence of quartz. Radiat. Meas. 42 (10), 1587–1599.
Pagonis, V., Baker, A., Larsen, M., Thompson, Z., 2011. Precision and accuracy of two luminescence dating techniques for retrospective dosimetry: SAR-OSL and SAR-ITL. Nucl. Instrum. Methods Phys. Res. B 269 (7), 653–663.
Peng, J., Li, B., 2017. Single-aliquot regenerative-dose (SAR) and standardised growth curve (SGC) equivalent dose determination in a batch model using the R package "numOSL". Anc. TL 35 (2), 32–53.
Peng, J., Pagonis, V., 2016. Simulating comprehensive kinetic models for quartz luminescence using the R program KMS. Radiat. Meas. 86, 63–70.
Peng, J., Wang, X.L., 2020. On the production of the medium component in quartz OSL: experiments and simulations. Radiat. Meas. 138, 106448.
Peng, J., Dong, Z.B., Han, F.Q., Long, H., Liu, X.J., 2013. R package numOSL: numeric routines for optically stimulated luminescence dating. Anc. TL 31 (2), 41–48.
R Core Team, 2019. R: a Language and Environment for Statistical Computing. R Foundation for Statistical Computing, Vienna, Austria. https://www.r-project.org.
Rhodes, E.J., Bailey, R.M., 1997. The effect of thermal transfer on the zeroing of the luminescence of quartz from recent glaciofluvial sediments. Quat. Sci. Rev. 16 (3–5), 291–298.
Roberts, H.M., Duller, G.A.T., 2004. Standardised growth curves for optical dating of sediment using multiple-grain aliquots. Radiat. Meas. 38 (2), 241–252.
Roberts, R.G., Galbraith, R.F., Olley, J.M., Yoshida, H., Laslett, G.M., 1999. Optical dating of single and multiple grains of quartz from Jinmium rock shelter, northern Australia: Part II, Results and implications. Archaeometry 41, 365–395.
Spooner, N.A., Questiaux, D.G., 2000. Kinetics of red, blue and UV thermoluminescence and optically-stimulated luminescence from quartz. Radiat. Meas. 32 (5–6), 659–666.
Thomsen, K.J., Murray, A.S., Bøtter-Jensen, L., 2005. Sources of variability in OSL dose measurements using single grains of quartz. Radiat. Meas. 39 (1), 47–61.
Wang, X.L., Peng, J., Adamiec, G., 2021. Extending the age limit of quartz OSL dating of Chinese loess using a new multiple-aliquot regenerative-dose (MAR) protocol with carefully selected preheat conditions. Quat. Geochronol., 101144
Wang, X.L., Wintle, A.G., Du, J.H., Kang, S.G., Lu, Y.C., 2011. Recovering laboratory doses using fine-grained quartz from Chinese loess. Radiat. Meas. 46, 1073–1081.
Wang, X.L., Du, J.H., Adamiec, G., Wintle, A.G., 2015. The origin of the medium OSL component in West Australian quartz. J. Lumin. 159, 147–157.
Weinstein, I.A., Popko, E.A., 2007. Evolutionary approach in the simulation of thermoluminescence kinetics. Radiat. Meas. 42 (4–5), 735–738.
Wintle, A.G., 1975. Thermal quenching of thermoluminescence in quartz. Geophys. J. Roy. Astron. Soc. 41, 107–113.
Wintle, A.G., Murray, A.S., 1998. Towards the development of a preheat procedure for OSL dating of quartz. Radiat. Meas. 29 (1), 81–94.
Wintle, A.G., Murray, A.S., 2006. A review of quartz optically stimulated luminescence characteristics and their relevance in single-aliquot regeneration dating protocols. Radiat. Meas. 41 (4), 369–391.
Zimmerman, J., 1971. The radiation-induced increase of the 100 $^{o}$C thermoluminescence sensitivity of fired quartz. J. Phys. C Solid State Phys. 4 (18), 3265–3276.